Black hole accretion disk diffuse neutrino background

T. S. H. Schilbach and O. L. Caballero*
Department of Physics, University of Guelph, Guelph, Ontario N1G 2W1, Canada

G. C. McLaughlin
Department of Physics, North Carolina State University, Raleigh, North Carolina 27695, USA

(Received 1 October 2018; published 9 August 2019)

We study the cosmic MeV neutrino background from accretion disks formed during collapsars and the coalescence of compact-object mergers. We provide updated estimates, including detection rates, of relic neutrinos from collapsars, as well as estimates for neutrinos that are produced in mergers. Our results show that diffuse neutrinos detected at HyperK would likely include some that were emitted from binary neutron-star mergers. The collapsar rate is uncertain, but at its upper limit relic neutrinos from these sources would provide a significant contribution to the cosmic diffuse neutrino background.

DOI: 10.1103/PhysRevD.100.043008

I. INTRODUCTION

Accretion disks surrounding black holes (BH) or hypermassive neutron stars (HMNS) are likely the final fate of the coalescence of a neutron star (NS) with a compact object (BH or NS) [1–5]. Accretion disks are also formed during rare supernovae (SN) that have significant rotation, termed collapsars [6–9]. During these events, much of the gravitational energy is released as neutrinos. The neutrinos are interesting not only because of their key role in the setting of the electron fraction and subsequent synthesis of elements, e.g., [10–14], or their suspected contribution to the triggering of long duration gamma-ray bursts (see, e.g., [15–19]), but also because they are one of the signals that come from these multimessenger objects. Even from a small number of neutrinos (just like in the SN1987 case [20]), much can be gleaned about the central engines of these objects.

Neutrinos emitted from these accretion disks are expected to be in the energy range of MeV. It is well known that astrophysical MeV neutrinos could be registered at existing facilities such as SuperKamiokande (SK) [21] and SNOLAB [22]. The prospects of detection in larger facilities like the proposed Hyperkamiokande, UNO, DUNE, JUNO, and TITAND [23–27], are even more promising [28,29]. There are two basic strategies for detecting these MeV neutrinos, either a direct detection from an object that is sufficiently close to produce a substantial flux at Earth, or a detection of the cosmic MeV neutrino background. The latter is formed by the accumulation of neutrinos from such objects over time. The consideration of the cosmic MeV neutrino background (CMNB) from all types of extragalactic sources (supernovae, collapsars, and binary mergers) enhances our chances of detection and opens a window to neutrino physics at cosmological scales. A detection of the CMNB will provide insights to the star formation history, initial mass function, cosmic metallicity, and event rates (see, e.g., [30,31]).

While many types of events can contribute to the CMNB, two types of events have been explored most extensively. Because of its promising prospects for detection, the supernova relic neutrino (SRN) background has been widely studied (e.g., [32–38]; for reviews see, e.g., [32,39]). SRN searches at SK have significantly improved upper limits, and they are now very close to predictions [40–42]. The next most studied contribution to the CMNB is that of relic neutrinos from failed supernovae [or unnovae (UN)]. Theoretical fluxes [30,43–46] have been found to be comparable to that of supernovae [47].

In this paper we add to previous CMNB studies by considering the neutrino background due to accretion disks from compact object mergers and supernovae (collapsars). We use updated models to extend previous work on collapsars, for example, that of [48], which found optimistic detection prospects for TITAND, using a neutrino background determined from the collapsar model in [49]. We also make the first determination of the diffuse neutrino background from compact object mergers. In both scenarios, matter surrounding the remnant black hole or hypermassive neutron star is hot and will emit considerable numbers of neutrinos. The study of the accretion tori allows for a determination of neutrino emission, *after* black hole formation, of collapsars and mergers. By considering two different accretion disk models, discussed later, we investigate the effect that the accretion rate and the BH spin have

*ocaballe@uoguelph.ca

on the neutrino spectra, on the relic background, and on the associated number of neutrinos reaching Earth's detectors.

The derivation of an accretion disk diffuse flux relies on two components: the neutrino spectra emitted in one of the above scenarios and the cosmological rate at which these events occur. In both collapsars and mergers, the neutrino emission can be comparable to or even larger than supernovae. Simulations of failed supernovae have shown that the neutrino emission may be larger than that of a protoneutron star [50,51]; one then can expect that this could also be the case in collapsars. In the case where the disk is formed after a merger, the neutrino emission from one event, although shorter in duration, can be 1 or 2 orders of magnitude more luminous than that of a supernova [52]. Similar to [48] we employ steady-state models of accretion disks where the disk is considered to be the result of a collapsar, but in addition we consider a dynamical model. Our estimates come from updated models, which include neutrino cooling, a range of black hole spin, and estimates of gravitational bending and redshifting on the part of the neutrinos. We assume that the BH has been already formed and matter, in a torus distribution, is accreted into it at a given rate. We also comment on the case of an accretion disk surrounding a hypermassive neutron star.

The other component, the cosmological failed supernova and merger rates, has been revisited in recent years, motivating also this study. From one side the detection of gravitational waves from mergers at observatories such as Advanced-LIGO has triggered an impressive effort to estimate the merger coalescence rates [53,54], with estimates in the range of 10^{-6}–10^{-3}/year per Milky Way Equivalent Galaxy (MWEG) for NS-NS mergers, and 10^{-8}–3×10^{-5}/year per MWEG for BH-NS mergers [55]. The recent detection of neutron-star mergers suggests a rate of 1540^{+3200}_{-1220} Gpc^{-3} yr^{-1} [56]. On the other side, recent *Swift* gamma-ray burst data [57,58] have been used to provide new estimates for star formation rates [59] and failed supernovae [60].

In this manuscript we convolve the accretion disk neutrino spectra from two different models, with current failed supernova and merger rates. In doing so, we provide an updated baseline for future studies on relic neutrinos from collapsars, the first estimates from mergers, and comparison between the two scenarios. We focus on the electron antineutrino relic flux, its contribution to the MeV neutrino background, and its possible detection at water Cherenkov facilities.

Although important, we do not consider neutrino oscillations in this work. Oscillations change the large energy contribution of the neutrino spectra resulting in a larger number flux of relic electron antineutrinos (see, e.g., [33,61]). Oscillations are expected to play a significant role in mergers and collapsars, e.g., [62–64] and we discuss the role of oscillations in the accretion disk relic neutrinos in future work.

This paper is organized as follows: in Sec. II we discuss the accretion torus models used and in Sec. III we present the corresponding results for the neutrino spectra. We continue by introducing the compact object mergers and failed supernovae rates used in this work and show our results for the relic neutrino flux for each scenario in Sec. IV. In Sec. V we provide neutrino event rates at SK and finally in Sec. VI we conclude.

II. DISK MODELS

The diverse emissions that could be observed from binary mergers and collapsars have significantly stimulated the study of accretion disks in the last decades. Models incorporate neutrino cooling and utilize a variety of different methods, which include treatments that are fully relativistic, Newtonian, hydrodynamical, steady state, and dynamical; a few examples include, e.g., [4,9,65,66]. In this work we make use of two different disk models. One is a fully relativistic steady-state model by Chen and Beloborodov [67], and the other one is from a pseudorelativistic hydrodynamical simulation from Just *et al.* [12]. Based on these two models we calculate the neutrino spectra and the corresponding diffuse background, aiming to set bounds on the number of neutrino events detected on Earth. We briefly summarize these two models below.

In the first model, from Chen and Beloborodov, the disk is arranged to depend on radius solely. Matter properties such as temperature, density, pressure, etc., are vertically averaged. We extend this one-dimensional model by assuming axial symmetry and estimating the vertical structure with a simple hydrostatic model. The disk is formed by a gas of nucleons, α-particles, electrons, positrons, photons, and neutrinos in nuclear statistical equilibrium (NSE). The gas and radiation pressures are at equilibrium. The model is fully relativistic and uses the Kerr metric to account for two values of the BH spin $a = Jc/GM^2 = 0$ and 0.95 (J is the total angular momentum and M the BH mass). The effects of three-dimensional magnetohydrodynamical turbulence are approximated as is usual via one viscosity parameter α [68]. In what follows, these models are labeled according to the BH spin: "C0" for $a = 0$ and "Ca" for $a = 0.95$. The mass of the BH is 3 $M_\odot$ and the alpha viscosity is given by $\alpha = 0.1$. Steady accretion is assumed, allowing us to study the effect of a constant mass accretion rate, $\dot{M}$, on the neutrino spectra. For this model, we have used values of $\dot{M} = 3$, 5, 7, and 9 $M_\odot$/s. Observations of short and long gamma-ray burst luminosities suggest a range of accretion values between 0.1 and 10 $M_\odot$/s [69]. Fully relativistic dynamical simulations of high entropy rotating stellar cores show that the accretion rate just before and after BH formation varies depending on the degree of rotation and may be as high as 45 $M_\odot$/s, although it decreases with time to values of 5 $M_\odot$/s [9]. Binary NS merger simulations find that the accretion rate can be 0.1–1 $M_\odot$/s [70], or as

large as 10 $M_\odot$/s [71]. Dynamical magnetized BHNS merger simulations have found that the rate varies between 0.1 to around 5 $M_\odot$/s [72], while [73,74] found accretion rates around 1 $M_\odot$/s.

For the second model, we use the simulation results of Just *et al.* [12] who studied the disk evolution, based on parameters extracted from hydrodynamical simulations of NS-NS and BH-NS mergers. Their work assumes the only merger result is BH-torus systems. The simulations are performed in Newtonian hydrodynamics and assume axisymmetry while ignoring the torus self-gravity due to its insignificance relative to the BH. Relativistic effects are introduced by using the Artemova-potential [75] to describe the BH gravitational field, with the BH spin and mass held fixed. The equation of state assumed the same particles as the Chen and Beloborodov model above, but included a heavy nucleus (^{44}Mn), all of them in NSE. The simulations in [12] begin with a BH and torus accreting onto it. The BH mass is 3 $M_\odot$ and the alpha viscosity was taken to be $\alpha = 0.02$. While the model describes the time evolution of the disk, however, we focus here on a representative time of $t = 20$ ms. In the framework of this torus model, two BH spins are considered $a = 0$, and 0.8. These models are labeled in this work according to the BH spin: J0 for $a = 0$ and Ja for $a = 0.8$.

While neutrino cooling is already included in the two models, we aim to calculate neutrino spectra and diffuse fluxes for distant observers; therefore, we use our results from previous work, where we performed a "postprocessing" of the tori's thermodynamical properties and found the last points of neutrino scattering, also known as the neutrino sphere. Details on the calculation and discussion on the results can be found in [52,76].

In the case of binary neutron-star mergers, fully general-relativistic simulations have shown that rapidly rotating merger remnants allow the formation of a HMNS (see, e.g., [77]). The lifetime of this HMNS depends at least on angular momentum transport, gravitational wave emission, the equation of state, and neutrino cooling. When the angular momentum transport is dominant the HMNS collapses into a BH; otherwise it collapses after neutrino cooling. The neutrino luminosities of the HMNS found by Sekiguchi *et al.* [78] with relativistic simulations, and by Lippuner *et al.* [79], who studied HMNS with their accretion disks and their evolution after collapse to BHs in pseudo-Newtonian gravity, are of the order of 10^{53} ergs/s. The simulations show that neutrino emission will continue after collapse decreasing from the initial values set by the HMNS. The order of magnitude of the luminosities is the same as our results for BH-AD used here [76].

III. NEUTRINO SPECTRA

Neutrinos produced in accretion disks (and supernovae) are trapped due to the highly dense matter of these environments. The neutrinos begin the free streaming regime at the neutrino sphere, and therefore the neutrino properties observed at any point in space above the neutrino surface are characterized by the thermodynamical properties of such surface. To calculate the neutrino spectra we consider the number of neutrinos that are emitted from a mass element on the neutrino surface of a black hole accretion disk (BH-AD) with energy E. The number spectrum of neutrinos emitted by one BH-AD is

$$\frac{dN(E)}{dE} = \frac{g_\nu c}{2\pi^2(\hbar c)^3}\iint dA f(E) dt, \tag{1}$$

where dt corresponds to the total emission time and $g_\nu = 1$. We assume that the emission of neutrinos by one mass element is isotropic and with the integral over the area we sum over all mass elements. The function $f(E)$ in Eq. (1) is the usual Fermi-Dirac distribution for fermions,

$$f(E) = \frac{E^2}{e^{E/T}+1}, \tag{2}$$

with T being the *local* temperature at the neutrino surface [34]. Such a neutrino "sphere" is determined by finding the distance z_ν, above the equatorial plane of the disk, such that the optical depth, $\tau = 2/3$,

$$\tau = \int_{z_\nu}^{\infty} \frac{1}{l_\nu(\rho, z')} dz', \tag{3}$$

with ρ and z being cylindrical coordinates, and $l_\nu(\rho, z')$ the neutrino mean free path. We consider neutrinos scattering from neutrons, protons, and electrons, as well as neutrino-antineutrino annihilation. Figure 1 shows the electron antineutrino surfaces for the Ca (with accretion rate 3 $M_\odot$/s) and Ja models. The inner surface corresponds

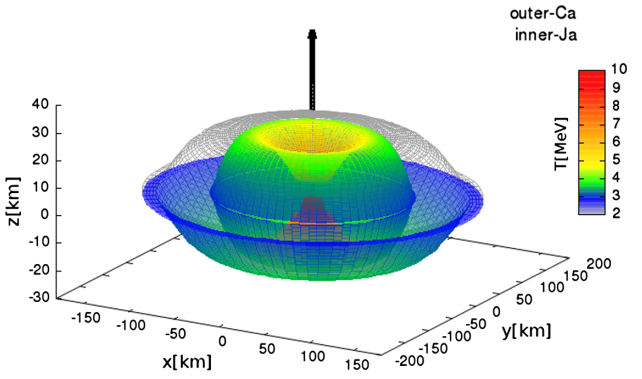

FIG. 1. Electron antineutrino surfaces for the steady-state model Ca with constant accretion rate 3 $M_\odot$/s (outer) and dynamical torus Ja (inner). The observer is on the symmetry axis of the disk. The upper half of the Ca neutrino surface is shown with lines to allow visualization of the Ja neutrino surface. The color scale indicates the local temperature at the antineutrino surface.

to the dynamical Ja model. We have used lines to plot the upper half of the electron antineutrino surface of the Ca model to allow visualization of the inner Ja surface. We assume that the observers are on the z axis at $r_o = z_o$, and that only neutrinos emitted from the upper half of the surface with cylindrical coordinates $(\rho_\nu,\ z_\nu)$, above the equatorial plane of the torus, will reach such observers. We are interested in the spectra seen by distant observers; therefore, their distance to the BH is much larger than the corresponding distance of the emitters ($r_\nu^2 = \rho_\nu^2 + z_\nu^2$), and the integral over the area is expanded as

$$\iint dA = \int_0^{2\pi} d\phi \int_{\rho_1}^{\rho_2} \rho d\rho, \tag{4}$$

where ρ_2, ρ_1, and ϕ are respectively the outer radius, inner radius, and angular component of the neutrino surface in cylindrical coordinates. Integrating over a flat surface introduces less than 10% error. We are mindful that it is the total flux emitted that is most relevant for the diffuse flux, so we check the adequacy of this approximation by comparing it with the flux that a distant observer would see if located on the plane of the disk, and we find a reduction of about $1/2$. We comment on the implications for neutrino detection in Sec. V.

As described up to this point, Eq. (1) corresponds to the neutrino spectrum as seen by a local observer (E and T as seen in the comoving frame of the disk). However, the spectrum observed at a distant point, $dN(E_\infty)/dE_\infty$, is affected by relativistic effects due to the strong gravitational field of the BH such as energy shifts, time dilation, and bending of neutrino trajectories. This means that if a disk is emitting neutrinos in a galaxy and is observed several kpc away the energy and time are redshifted as $E = (1 + z_{\rm BH})E_\infty$, $dt = (1 + z_{\rm BH})dt_\infty$, and the toroidal neutrino surface would appear larger by $dA_\infty = (1 + z_{\rm BH})^2 dA$, with $(1 + z_{\rm BH})$ being the redshift due to the BH (calculated accordingly to the distances r_o and r_ν).

The emission time varies according to the formation scenario of the disk. The J models correspond to mergers. The steady-state models could be suitable for mergers or collapsars depending on the accretion conditions. Dynamical simulations from the initial formation followed by long-term evolution would be needed to have accurate emission times and spectra, but such simulations are challenging. Therefore, we provide two estimates of the total emission time dt_∞ [76] (noted there as Δt_∞). In our first estimate, the maximum binding energy method, the time intervals are based on the efficiency ε to convert gravitational energy E_G into neutrino energy E_ν^B. The radiation energy efficiency, $\varepsilon = 1 - \tilde{E}$, depends on the BH spin a as

$$a = -\frac{4\sqrt{2}(1 - \tilde{E}^2)^{1/2} - 2\tilde{E}}{3\sqrt{3}(1 - \tilde{E}^2)}, \tag{5}$$

with $1 - \tilde{E}$ being the maximum binding energy at the marginally stable circular orbit (see, e.g., [80] for a discussion). With a rest mass energy $E_G = M_T c^2$, where M_T is the torus mass, we estimate $dt = E_\nu^B/L_\nu = \varepsilon E_G/L_\nu$, with L_ν being the neutrino luminosity. The mass is found by integrating the matter density over the disk volume. In this way, for the steady-state model Ca, with $a = 0.95$, and $\dot{M} = 9\ M_\odot/\mathrm{s}$ we find $\varepsilon = 0.19$, and $dt_\infty = 0.57$ s, corresponding to a torus mass of $1.36\ M_\odot$. This time changes with accretion rate and spin reaching to 0.34 s in the case of a torus with zero spin, accretion rate of $3\ M_\odot/\mathrm{s}$, and a mass of $0.136\ M_\odot$. For the dynamical disk, using this method and taking the reported simulation value of $M_T = 0.3\ \mathrm{M}_\odot$ [12], we find that the time interval is ~0.02 s. A second estimate for the signal duration is obtained by $dt = M_T/\dot{M}$. Note that this assumes that neutrino emission would be present during the full time of evolution (neutrino emission times could therefore be shorter). In the case of steady-state disks we find, for example, for Ca with $\dot{M} = 9\ M_\odot/\mathrm{s}$, $dt_\infty = 0.16$ s, while for C0 with $\dot{M} = 3\ M_\odot/\mathrm{s}$, $dt_\infty = 0.15$ s. In the case of the dynamical J models we estimated the accretion rate from the mass difference at two snapshots resulting in $dt \sim 0.2$ s. Note that Just *et al.* reported neutrino emission time of 250 ms for this particular torus, and that the neutrino-dominated accretion phase of their disks can vary between 0.1 and 1 s. Other authors (see, e.g., [81]) estimate shorter neutrino emission times for mergers of the order of 50 ms. With the aim of setting bounds for the diffuse flux, we take two limiting values for the signal duration, 20 ms and 2 sec, when considering the dynamical tori. For the steady-state disks applied to the collapsar scenario we take as lower limit the time found by $dt = M_T/\dot{M}$ and as an upper value the time estimate based on maximum efficiency for a given BH spin [Eq. (5)]; while when considering mergers evolving into these disks we take the $dt = M_T/\dot{M}$, which provide shorter emission times consistent with the formation scenario.

Taking into account the above strong gravitational field effects and the conservation of phase-space density, we generate the spectra observed far away from the source. In what follows we focus on electron antineutrinos only as we aim to calculate detection rates at water-based Cherenkov detectors. Figure 2 shows the results for electron antineutrinos using the steady-state and the hydrodynamical tori and compares with a protoneutron star spectrum [33,82]. In Fig. 2 we have used an accretion rate of $\dot{M} = 3\ M_\odot/\mathrm{s}$ for the Ca and C0 models and a signal duration estimated as above, $dt = \varepsilon E_G/L_\nu$. As can be seen, the disk spectra are larger than the SN one (from [82]), except for the C0 model, which is larger only for energies below $E < 14$ MeV. These results are consistent with the fact that accretion disks formed during mergers may result in higher neutrino emission temperatures than those of SN. On the other hand, if the disk is a result of a collapsar the results are also consistent with the fact that the formation of

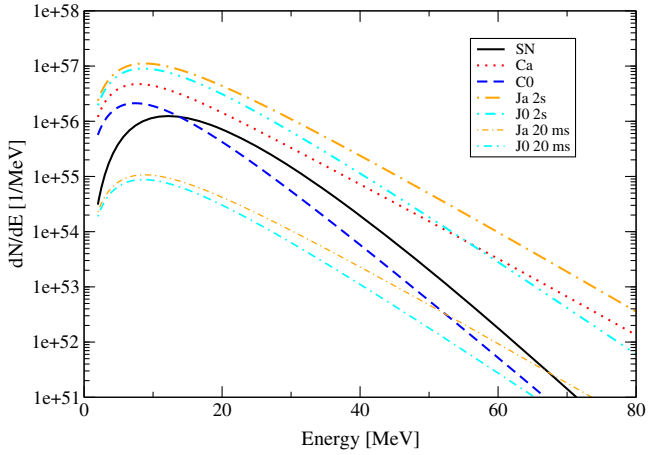

FIG. 2. Comparison of electron antineutrino spectra for the steady-state (C0, Ca with constant accretion rate 3 $M_\odot$/s) and dynamic tori (J0, Ja). The a indicates a large BH spin (see the text). In both disk models the BH mass is 3 $M_\odot$. The SN spectrum is shown for comparison.

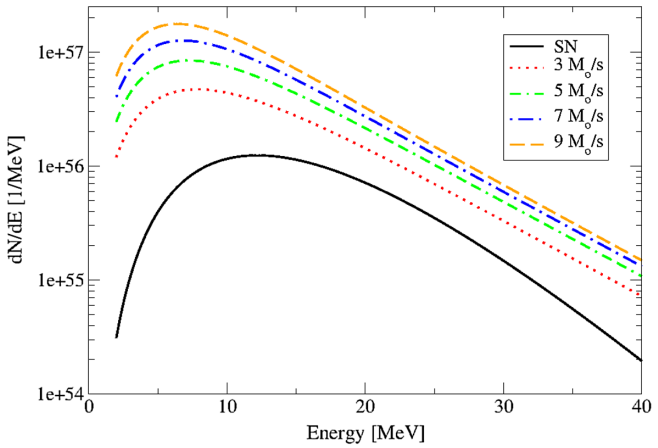

FIG. 3. The effect of the mass accretion rate on the AD electron antineutrino spectra for the steady-state Ca model (BH spin $a = 0.95$).

a BH (instead of a NS) creates a situation where, depending on the accretion rate, significant energy can become available for conversion to neutrino emission. In the C0 model with $\dot{M} = 3\ M_\odot$/s, although the highest neutrino temperature is $T = 4.3$ MeV (close to the well-known SN value of 5 MeV), the range of temperatures at the neutrino surface is below that of a SN. In contrast, at the same accretion rate, the change to a spinning BH (Ca model, described in the Kerr metric) generates hotter disks with larger angular momentum and inner edges closer to the BH where most of the power is released. The energy is transferred via viscous heating and then converted to neutrino energy. Similarly, for the hydrodynamical models, we find that the Ja torus has a larger neutrino spectrum compared to the J0 model, particularly at high energies.

In the case of accretion rate dependence, as shown in Fig. 3 for the Ca models, a similar conclusion is drawn: the larger the rate at which mass plunges into the BH the higher the temperature of the disk [67] and, therefore, the number of antineutrinos emitted per energy interval. As a result, a torus with a high accretion rate will have a stronger signal than a slower accreting disk [76].

Finally, comparing our results to those of Refs. [48,49] who use a collapsar model, we find that their neutrino emission is smaller. It is important to note that in their work, the authors modeled the disk as an advection-dominated flow, whereas the models presented here both allow for a neutrino-dominated phase. Also, other parameters such as a smaller accretion rate (0.1 $M_\odot$/s) and lower temperatures contribute to the differences. This, of course, has implications on the diffuse neutrino flux as discussed later.

The higher temperatures of accretion disk tori are similar to those from failed SN [83,84]. However, the overall magnitude of the failed SN spectra of [83,84] is smaller than our collapsar results. This is primarily because that case involves spherically symmetric matter distributions and neutrino emission only up to the onset of the BH, whereas in the models we employ the disk evolution and its neutrino emission corresponds to the period after BH formation.

IV. DIFFUSE FLUX

One single torus emits neutrinos according to the spectra found in the previous section. To find the disk diffuse neutrino background, we should consider the total number of disks that have emitted neutrinos from the past to the present time, and convolve it with the cosmologically redshifted neutrino spectrum. The number of disks, formed at a fixed time in the past, depends on the event rate $R(z_C)$ (number density of scenarios ending in a torus per unit time), which changes with the cosmological redshift z_C. This rate has to be transformed to account for the expansion of the Universe. In this way, we have that the present number density of BH-AD neutrinos, observed now between the energy interval $E_o + dE_o$, emitted in the redshift interval $z_C + dz_C$ is given by

$$\frac{dn_\nu(E_o)}{dE_o} = (1+z_C)R(z_C)\frac{dt_C}{dz_C}dz_C\frac{dN(E_\infty)}{dE_\infty}, \quad (6)$$

where $dN(E_\infty = (1+z_C)E_o)/dE_\infty$ is the number spectrum of neutrinos emitted by a single BH-AD, E_o is the registered energy on Earth and redshifted from E_∞. The last two energies are related by $E_\infty = (1+z_C)E_o$.

The Friedmann equation gives the relation between the past time t_C and z_C as

$$\frac{dt_C}{dz_C} = -1/(H_0(1+z_C)(\Omega_m(1+z_C)^3 + \Omega_\Lambda)^{1/2}), \quad (7)$$

where $\Omega_m = 0.3$, $\Omega_\Lambda = 0.7$, and $H_0 = 70$ km/s/Mpc in the ΛCDM standard cosmology (see, e.g., [85]).

The differential number flux of BH-AD diffuse neutrinos, $dF/dE_o = c dn_\nu/dE_o$, with c being the speed of light, is obtained by summing over the cosmological redshift,

$$\frac{dF}{dE_o} = -c \int_0^{z_{\max}} (1+z_C) R(z_C) \frac{dN(E_\infty)}{dE_\infty} \frac{dt_C}{dz_C} dz_C, \quad (8)$$

where $z_{\max}$ is the maximum cosmological redshift considered, and $dN(E_\infty)/dE_\infty$ is the transformed spectrum in terms of the observed energy on Earth, E_o. Therefore, two primary redshifts were factored into this work, both from cosmological expansion and from the escape from the parent BH.

A key ingredient in our calculation is the event rate $R(z_C)$, which changes with the cosmological redshift and depends on the scenario considered. Based on the BH-AD progenitor rate, $R(z_C)$, we calculate diffuse neutrino fluxes dF/dE_o for the mergers and collapsar scenarios. Before presenting our results for the diffuse flux we discuss the event rates $R(z_C)$ used in this work.

A. Compact object merger rates

For our study of disk formation in the merger scenario we use the results of Dominik *et al* for extragalactic compact object merger rates [54,86]. The corresponding rates at $z_C = 0$ are consistent with the lower limit inferred from the recent observation of gravitational waves from a NS-NS merger [56]. It should be noted that Dominik *et al.*'s work corresponds to field stellar populations only and therefore their results, and the ones obtained here based on those, are a conservative lower limit, as mergers occurring in globular clusters increase such rates. Their results for black hole-neutron star (BH-NS), neutron star-neutron star (NS-NS) are shown in Fig. 3 of [54], and we plot them here to provide context. Their merger rates were broken into four distinctive approaches to merger modeling: their standard baseline model, their optimistic common envelope model, which allows for envelope donors, delayed SN model without a rapid SN engine, and high BH kicks with BHs providing full natal kicks.

For the purpose of analyzing the most optimistic and pessimistic cases within this data set, we plot upper and lower limits in Fig. 4. The upper limits for BH-NS and NS-NS correspond to the galactic low-end metallicity with common envelope merger scenario (labeled here as Opt. BH-NS) and NS-NS (Opt. NS-NS). The pessimistic cases are the high-end metallicity evolution scenario with BH kicks for BH-NS (in this work labeled as Pes. BH-NS) and the low-end metallicity evolution scenario with the standard merger model of [54] for NS-NS (here Pes. NS-NS). The two lines labeled as Stand. correspond to the high-end metallicity evolution in the standard model for BH-NS and NS-NS.

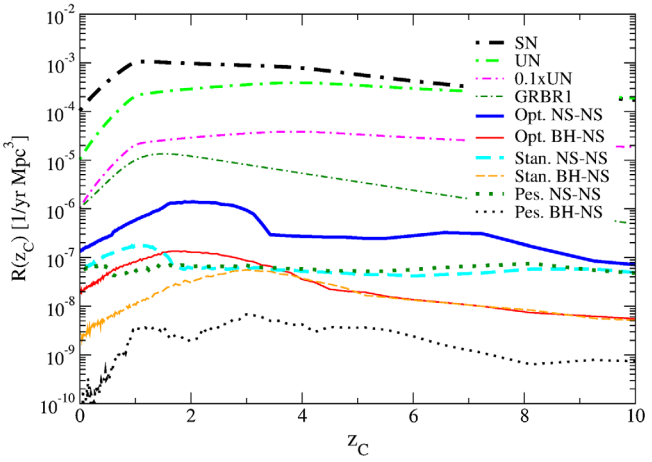

FIG. 4. Comparison of optimistic, standard, and pessimistic cosmological BH-NS and NS-NS merger rates (from [54]). The SN and failed SN or UN rate are as proposed in [60]. The 0.1×UN line assumes that only 10% of the UN would form a disk. GRBR1 is the collapsar rate as proposed in [48].

B. Supernovae rates

The SN rates are gathered from the results of Yüksel and Kistler [60], which utilize an updated star formation history fit from Kistler *et al.* [87] based upon the original star formation rate fit done by Yüksel *et al.* [59],

$$R_{SN} = \zeta \dot{\rho}_o \left((1+z_C)^{a\eta} + \left(\frac{1+z_C}{B}\right)^{b\eta} + \left(\frac{1+z_C}{C}\right)^{c_1\eta} \right)^{1/\eta}, \quad (9)$$

where $a = 3.4$, $b = -0.3$, $c_1 = -2$, $\eta = -10$, $B \simeq 5100$, $C \simeq 14$, $\dot{\rho}_o = 0.014\ M_\odot/\mathrm{yr\,Mpc^3}$, and $\zeta = 0.0074/M_\odot$ [60,87]. To modify this rate for the particular case of failed SN, it is multiplied by

$$(1+z_C)/10, \quad (10)$$

as discussed in Yüksel *et al.* [60]. This factor is a consequence of indications, given by bright gamma-ray burst observations, that the failed supernova rate may evolve with a higher dependency of the cosmological redshift by a factor of $(1+z_C)$ [88]. The factor scales with z_C due to the theoretical expectation that lower metallicity stars will generate more massive cores. The above parametrization of SN rates comes with the assumption that every star over 8 $M_\odot$ experiences a core collapse, and uses a Salpeter mass function that continues up until 100 $M_\odot$, and further that 10% of supernovae are unnovae and do not produce a supernova light curve. We view this failed supernova rate as an upper limit to the number of supernova that could form accretion disks, as the fraction is relatively unconstrained. However, we must keep in mind that the true fraction could be smaller. The failed SN rate is shown in Fig. 4 with the thick light-green dot-dashed line. Recent simulations have

shown that massive stars with low metallicity and low mass loss can evolve into a black hole with a disk [89]. Also, Sekiguchi *et al.* [9] studied the evolution of high-entropy rotating stellar cores and found that even in the case of a slowly rotating core the system evolves into a BH with a thin disk. Therefore, the fraction of black hole forming collapses that lead to a disk could be a substantial fraction of the failed supernova rate. Nevertheless, to account for this uncertainty, we also provide estimates assuming that only 10% of the failed SN would form a disk (magenta dot-dashed line). For comparison the lowest estimate for collapsar rates of [48], GRBR1, is also shown (thin dark-green dot-dashed line).

C. Diffuse flux results

We make estimates for the number flux of neutrinos based on Eq. (8) for each astrophysical scenario. Figure 5 shows the diffuse fluxes for electron antineutrinos when the spectrum corresponds to a disk with a 3 $M_\odot$/s accretion rate (Ca model) and with a signal duration based on maximum efficiency as Eq. (5). It can be seen that the upper limit for the collapsar relic flux (dashed orange line) is comparable to that of a SN (dotted-dashed black line). Based on our results of neutrino spectra (Figs. 3 and 2), it follows that the upper limit on the collapsar diffuse background will be larger than the SN one for the 9 $M_\odot$/s Ca disk, and lower in the 3 $M_\odot$/s C0 case. Therefore, for the accretion rates and BH spin ranges considered in this work, there exists the possibility that the number of neutrinos detected may be comparable to that of the diffuse SN background. This is because, although the unnova rate is an order of magnitude lower than the SN rate, the binding energy available for neutrino emission in disks from collapsars is larger than the one in a SN.

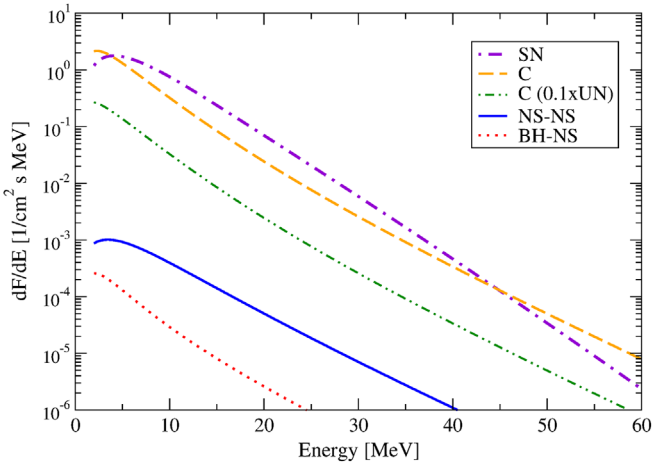

FIG. 5. Comparison of supernova (SN), collapsar upper limit (C), collapsar with 10% unnova rate (C(0.1 × UN)), BH-NS, and NS-NS accretion disks diffuse neutrino fluxes where the accretion rate is 3 $M_\odot$/s and the BH spin is $a = 0.95$ (steady-state model).

Our results in the collapsar model for the diffuse background are significantly larger than those found by Nagataki *et al.* [48]. This is in part due to an increased neutrino emission, and in part due to the using the unnovae rate as an upper limit on the collapsar flux (see Fig. 4). As discussed above the fraction of BH forming collapses that evolve into a disk is still unknown. However, if this fraction is not of orders of magnitude smaller than the unnovae, then the diffuse neutrino flux in the collapsar scenario would contribute in a meaningful way to the CMNB. The green double dotted-dashed line in Fig. 5 presents results where we have assumed that only 10% of the failed supernovae would form a disk.

We also plot in Fig. 5 the contribution from NS-NS mergers and BH-NS mergers. As expected because of larger anticipated rates (see Fig. 4) NS-NS mergers provide consistently greater contributions to the differential flux than the BH-NS, because of their larger rate of occurrence.

V. DETECTION RATES

The number of diffuse electron antineutrinos registered in a given facility per year, R_D, is obtained by integrating Eq. (8) with the detector cross section, $\sigma(E_o)$,

$$R_D = N_T \int_{E_{th}} \sigma(E_o) \frac{dF}{dE_o} dE_o. \tag{11}$$

Here N_T is the number of targets in the detector, E_{th} is its corresponding energy threshold, E_o is the energy at the lab, and dF/dE_o is the diffuse flux discussed in Sec. IV.

For water-based Cherenkov detectors the relevant reaction is

$$\bar{\nu}_e + p \to e^+ + n, \tag{12}$$

where the cross section is given by

$$\sigma_{\bar{\nu}_e p \to n e^+} = \frac{\sigma_0}{4m_e^2}(1 + 3g_A^2)(E_o - \Delta)^2 \times \left[1 - \left(\frac{m_e}{E_o - \Delta}\right)^2\right]^{1/2}, \tag{13}$$

with $\sigma_0 = 4G_F^2 m_e^2/(\pi\hbar^4)$, $g_A = 1.26$, m_e being the electron mass, $\Delta = 1.293$ MeV the neutron-proton mass difference, and G_F the Fermi coupling constant.

Figures 6 and 7 show the change with electron antineutrino energy on Earth, dR_D/dE_o, when the accretion disk is formed during collapsars, and BH-NS and NS-NS mergers, in SK assuming a 32 kton fiducial volume. In order to study lower and upper limits of R_D, we have considered the most optimistic and pessimistic formation scenarios, together with the strongest and weakest neutrino spectra. For collapsars, we take the optimistic and pessimistic collapsar rates and fold them together with a range of neutrino emission models. These generate the extremes of

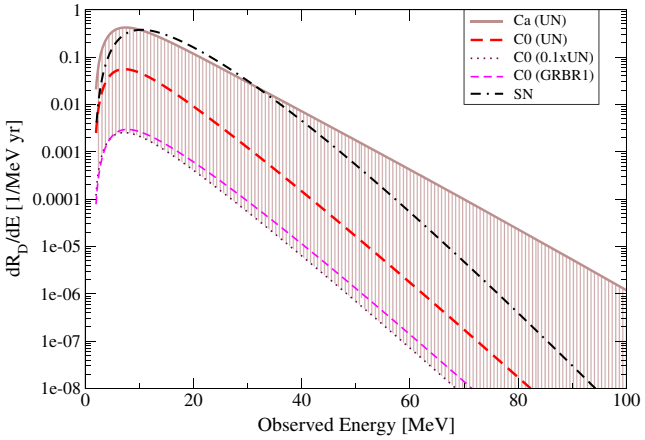

FIG. 6. Event rate per MeV per year in SK for the BH-AD diffuse neutrino background in the collapsar scenario. Optimistic (UN) and pessimistic ($0.1 \times$ UN) limits as per rate estimates are shown in Fig. 4. The SN and results combining the C0 model with GRBR1 rates from [48] are shown for comparison.

the band shown in Fig. 6. In this way, in the collapsar scenario, the upper brown solid line corresponds to convolving the failed supernova rate with a electron antineutrino spectrum coming from a (Ca) disk accreting at a rate of 9 $M_\odot/$ sec, a BH spin $a = 0.95$, and emitting neutrinos for $dt_\infty \approx 0.57$ secs [the emission time found assuming maximum efficiency, Eq. (5), as described in Sec. III]; while the brown dotted line convolves a $0.1\times$ unnova rate with a disk accreting at 3 $M_\odot/$ sec into a BH with a spin $a = 0$ and emitting for 0.15 s (lower limit estimated at the given accretion rate). For comparison we also show the detection rates found for the C0 disk model emitting for 0.34 s with the optimistic UN rate (thick red dashed line) and the collapsar rate, GRBR1, from Nagataki *et al.* [48] (thin magenta dashed line).

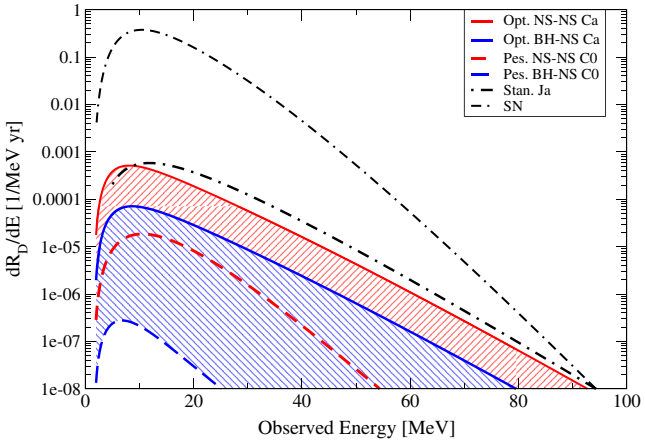

FIG. 7. Event rate per MeV per year in SK for the BH-AD diffuse neutrino background in the merger scenarios. Optimistic and pessimistic limits as per rate estimates are shown in Fig. 4. The SN results are shown for comparison.

We proceed in a similar fashion to evaluate the limiting lines of Fig. 7 in the merger scenarios. There, for the spectra, we have considered signal durations given by the accretion rate $M_T/\dot{M}$ and tori with masses less or equal to 1 $M_\odot$ to be consistent with the merger formation scenario. The longer times estimated with maximum efficiency would predict torus masses that exceed the initial total premerger mass, and tori with larger masses would surpass the observational constraint of 2 $M_\odot$ for a NS. The formation of 1 $M_\odot$ tori with a 3 $M_\odot$ BH is statistically not the most likely scenario, so we considered it here as an optimistic scenario. Exploring a series of models with different BH masses could be done in future work. With this in mind, our optimistic estimate corresponds to neutrinos emitted from a Ca 7 $M_\odot/$s disk model during 0.173 s, while the lower limit corresponds to a C0 model accreting at 3 $M_\odot/$s during 0.15 s.

For the merger rates we use the optimistic and pessimistic occurrence rates as discussed in Fig. 4. Therefore, the red solid line in Fig. 7 is found by multiplying the Ca spectrum ($\dot{M} = 7\ M_\odot/$s) with a NS-NS merger rate calculated assuming a galactic low-end metallicity evolution and the development of a common envelope during the compact object merger (see the blue thick line in Fig. 4). The pessimistic NS-NS neutrino detection rate in Fig. 7 (red dashed line) assumes that neutrinos have been emitted from C0 disks with an accretion rate of 3 $M_\odot/$s and occurring in galaxies with low metallicity and in the standard merger model of Dominik *et al.* (green thick dotted line in Fig. 4). Finally, for the BH-NS merger, the optimistic neutrino detection rates (blue solid lines) correspond to a low-end metallicity galactic evolution with common envelope for the BH-NS merger that evolves into the Ca disk model with $\dot{M} = 7\ M_\odot/$ sec, while the pessimistic detection (blue dashed line) corresponds to a spectrum from a C0 disk with $\dot{M} = 3\ M_\odot/$s and a BH-NS rate in the high-end metallicity evolution scenario with the merger producing BH kicks. All other evolution scenarios and conditions that change the neutrino flux (e.g., accretion rates), considered here, fall inside these bands for the Chen-Beloborodov models. The black dot-dashed line shows the detection rate obtained for the hydrodynamical model Ja with an estimated emission time of 2 sec, considering the torus was the result of a NS-NS merger (in the standard evolution scenario) happening in a galaxy with high metallicity. It is clear from the figure that if the collapsar formation rate is high, then the dominant component to the detection rates comes from collapsars, followed by a disk formed during a NS-NS merger, and finally there are, due to the low occurrence rates, the BH-NS disks.

The total number of relic neutrinos per year is obtained after integrating dR_D/dE_o with energy interval starting from the energy threshold of SK, 5 MeV, up to 100 MeV. The integrated rates, as per Eq. (11), are written in Table I, where we also report the estimates found for the Ja and J0

TABLE I. Rate of relic neutrinos (1/yr) at SK (32k ton) and HK (560 kton) for the scenarios considered in Figs. 6 and 7 with formation rates as in Fig. 4.

Scenario	Formation rate	Disk model	$\dot{M}$ ($M_\odot$/s)	R_D SK (1/yr)	R_D HK (1/yr)
Collapsar	UN	Ca	9	5.2	91
	0.1xUN	C0	3	0.02	0.35
NS-NS merger	Opt.	Ca	7	7.0×10^{-3}	0.12
	Pes.	C0	3	2.7×10^{-4}	0.004
	Opt.	Ja	⋯	3.3×10^{-2}	0.57
	Pes.	J0	⋯	4.5×10^{-3}	0.08
	Stan.	Ja	⋯	1.0×10^{-2}	0.17
BH-NS merger	Opt.	Ca	7	1.0×10^{-3}	1.7×10^{-2}
	Pes.	C0	3	2.4×10^{-6}	4.2×10^{-5}
	Opt.	Ja	⋯	4.7×10^{-3}	8×10^{-2}
	Pes.	J0	⋯	4.4×10^{-5}	8×10^{-4}

models assuming a signal of 2 s. (J0 is not shown in Fig. 7 for clarity). The tabulated cases correspond to the same cases in Figs. 6 and 7, which, as expected from Figs. 2, 3, and 5, show significant increases in detection rates stepping from BH-NS to NS-NS and to the collapsar case. We also provide rescaled results for the 560 ktons of HyperK.

In Table II we summarize our detection rates for the diffuse neutrino background when the neutrino spectra correspond to steady-state disks (C models). The results for collapsars (left column) assume an emission time given by maximum efficiency of converting gravitational energy to neutrino energy. However, this time can be shorter as there are other kinds of emissions. For the merger results (right column) the emission time is based on the total mass of the disk and the accretion rate. We warn that a study of the long-term evolution of mergers predicts lower disk mass that the ones we find here [90]. The spectra were convolved with the UN rates and with the NS-NS merger rates in the standard coalescence scenario in galaxies with high-end metallicity. The increased changes in detection are related to the increase in accretion rate and BH spin. For comparison we have included the results for the diffuse SN background found when we take the SN rates as in Eq. (9) and consider a SN spectrum as in Ref. [82]. We show neutrino counts for two energy windows, one above SuperK threshold, from 5 to 100 MeV, and another one that corresponds to the current allowed interval, above detector backgrounds (atmospheric and reactor backgrounds), from 11 to 30 MeV.

TABLE II. Number of relic neutrinos per year, R_D, from collapsars and NS-NS mergers, assuming the remnant disks accrete with a fixed rate $\dot{M}$ and BH spin a. Rates are given for two sets of energy windows in Super-K. Results for SN are provided for comparison.

$E_{\bar{\nu}_e} > 5$ MeV				
R_D [1/yr]	Collapsar		NS-NS ($\times 10^{-3}$)	
$\dot{M}$	$a = 0$	$a = 0.95$	$a = 0$	$a = 0.95$
3 $M_\odot$/s	0.5	2.3	0.4	1.7
5 $M_\odot$/s	0.8	3.4	0.7	2.1
7 $M_\odot$/s	1.0	4.4	0.8	2.3
9 $M_\odot$/s	1.3	5.2	⋯	⋯
SN	5.3			
$11 < E_{\bar{\nu}_e} < 30$ MeV				
3 $M_\odot$/s	0.2	1.2	0.23	1.1
5 $M_\odot$/s	0.3	1.8	0.4	1.3
7 $M_\odot$/s	0.4	2.3	0.5	1.4
9 $M_\odot$/s	0.5	2.6	⋯	⋯
SN	3.3			

Note that our results depend linearly with emission time (time dilation has been taken into account in the redshift $1 + z_{\rm BH}$) and can be rescaled for the same BH mass. Also, as discussed in Ref. [76] and mentioned in Sec. III, neutrino properties depend on the observer's inclination. The results we have reported here assumed that the observer is located on the z axis. If we instead estimate the emission from the disks assuming the observer is on the equatorial plane of the disk, and neutrinos emerged *only* from the right half of the neutrino surface, we would find a dR_D/dE reduced by a factor of ∼0.6 for neutrinos with energies around 10 MeV (based on Ca model with 5 $M_\odot$/s). One could expect a similar trend for other disks. However, this estimate does not take into account that for such observers trajectory bending can be sufficiently strong for a detector to register neutrinos emitted from the back of the disk, or even from places close to the BH emerging but from the opposite side of the surface, which enhances the number of neutrinos detected.

VI. SUMMARY AND CONCLUSIONS

We have studied the spectra, diffuse fluxes, and detection rates in SuperK and HyperK, of neutrinos emitted by past to

present black hole accretion disks. Those are considered to be one of the possible final fates of rotating core collapse supernovae, as well as of mergers of neutron stars with black holes or with other neutron stars. The models used for our study include important aspects such as neutrino cooling and relativistic effects.

Neutrino disk spectra depend on the mass accretion rate and the BH spin. The evolution of accretion disks is such that there is a funnel formed around the black hole. When neutrinos are emitted from that low density region they have large temperatures. The effect of these high temperatures and the toruslike geometry is reflected in a hotter neutrino spectrum compared to that from spherically symmetric SN simulations (the latter are used to study the failed SN spectrum). The number of failed supernovae that evolve into a disk (in a collapsar model) depends on still to be determined physics such as the nuclear matter equation of state and the progenitor initial conditions, leaving us with open questions on the mechanism of BH formation. Future simulations would shed light into the BH mass, BH spin, emission time, and accretion rate ranges that would be possible if such tori formed from unsuccessful SN.

This uncertainty notwithstanding, our spectra results motivated us to study the potential contribution of these neutrinos to the relic neutrino background in the MeV range. We find that in the collapsar model, assuming an upper limit event rate that is the same as the unnova rate, this diffuse flux is comparable (larger for high mass accretion rates) to the SN one. We find that the number of neutrinos registered in SuperK (taking an energy threshold of 5 MeV) in a 5-year period from collapsars would be between 3 and 25. As discussed elsewhere (see e.g., [43]), the atmospheric and reactor neutrino fluxes limit the detection energy window from $\sim$11 to 30 MeV in the current SuperK setup. In that range we predict that in the most optimistic collapsar model we will find about three counts per year.

We also studied the diffuse flux and possible detection of neutrinos coming from ADs in the scenario where the torus was the result of a neutron star-compact object merger. The cosmological merger rates lead to diffuse fluxes that are at least 2 orders of magnitude smaller than those of SN and collapsars. However, the upgrade from SuperK to HyperK will allow for a detection of at least one of those neutrinos (in the most optimistic merger scenario) in a period of 1.75 years. It is important also to keep in mind that these results are based on merger rates for field stellar populations [54], but rates should be larger in globular clusters. The rates are also sensitive to parameters in the binary model and initial distributions of the binary [91]. A recent compilation of different predictions of NS-NS and BH-NS merger rates can be found in [92] showing that event rates may be higher than assumed here.

The prospects of overcoming the current detection limitations on the detection of the CMNB are promising. Extracting relic neutrino signals in SK, with more data collected, improved efficiency, and lower threshold will be a reality in few years [42]. The possibility of a megaton water-Cherenkov detector like HyperK opens the door to significant numbers of diffuse neutrinos being observed. In analyzing such a future detection, we should bear in mind that in addition to standard core collapse and failed supernovae, a few of these neutrinos may come from accretion disk supernovae and compact object mergers.

ACKNOWLEDGMENTS

We thank the referee for insightful comments and careful revision of the manuscript. O. L. C. thanks Eric Poisson for useful discussions. This work was partially supported by the Natural Sciences and Engineering Research Council of Canada (NSERC) (O. L. C.), the U.S. DOE Grant No. DE-FG02-02ER41216, and the National Science Foundation, Grant No. PHY-1630782 (G. C. M.).

[1] W. Kluzniak and W. H. Lee, Mon. Not. R. Astron. Soc. **308**, 780 (1999).
[2] S. Rosswog, Astrophys. J. **634**, 1202 (2005).
[3] C. L. Fryer, K. Belczynski, E. Ramirez-Ruiz, S. Rosswog, G. Shen, and A. W. Steiner, Astrophys. J. **812**, 24 (2015).
[4] F. Foucart, M. B. Deaton, M. D. Duez, E. O'Connor, C. D. Ott, R. Haas, L. E. Kidder, H. P. Pfeiffer, M. A. Scheel, and B. Szilagyi, Phys. Rev. D **90**, 024026 (2014).
[5] L. Lehner, S. L. Liebling, C. Palenzuela, O. L. Caballero, E. O'Connor, M. Anderson, and D. Neilsen, Classical Quantum Gravity **33**, 184002 (2016).
[6] A. MacFadyen and S. E. Woosley, Astrophys. J. **524**, 262 (1999).
[7] E. O'Connor and C. D. Ott, Astrophys. J. **730**, 70 (2011).
[8] C. D. Ott, C. Reisswig, E. Schnetter, E. O'Connor, U. Sperhake, F. Löffler, P. Diener, E. Abdikamalov, I. Hawke, and A. Burrows, Phys. Rev. Lett. **106**, 161103 (2011).
[9] Y. Sekiguchi and M. Shibata, Astrophys. J. **737**, 6 (2011).
[10] R. Surman and G. C. McLaughlin, Astrophys. J. **603**, 611 (2004).
[11] R. Surman and G. C. McLaughlin, Astrophys. J. **679**, L117 (2008).

[12] O. Just, A. Bauswein, R. A. Pulpillo, S. Goriely, and H.-T. Janka, Mon. Not. R. Astron. Soc. **448**, 541 (2015).
[13] O. L. Caballero, G. C. McLaughlin, and R. Surman, Astrophys. J. **745**, 170 (2012).
[14] R. Surman, G. C. McLaughlin, M. Ruffert, H.-T. Janka, and W. R. Hix, Astrophys. J. **679**, L117 (2008).
[15] S. E. Woosley, Astrophys. J. **405**, 273 (1993).
[16] R. Popham, S. E. Woosley, and C. Fryer, Astrophys. J. **518**, 356 (1999).
[17] A. Murguia-Berthier, E. Ramirez-Ruiz, G. Montes, F. De Colle, L. Rezzolla, S. Rosswog, K. Takami, A. Perego, and W. H. Lee, Astrophys. J. **835**, L34 (2017).
[18] J. P. Kneller, G. C. McLaughlin, and R. Surman, J. Phys. G **32**, 443 (2006).
[19] T. Liu, W. M. Gu, and B. Zhang, New Astron. Rev. **79**, 1 (2017).
[20] K. Hirata *et al.* (Kamiokande-II Collaboration), Phys. Rev. Lett. **58**, 1490 (1987).
[21] S. Fukuda *et al.*, Nucl. Instrum. Methods Phys. Res., Sect. A **501**, 418 (2003).
[22] F. Descamps (SNO+Collaboration), Nucl. Part. Phys. Proc. **265–266**, 143 (2015).
[23] K. Nakamura, Int. J. Mod. Phys. A **18**, 4053 (2003).
[24] C. K. Jung, AIP Conf. Proc. **533**, 29 (2000).
[25] R. Acciarri *et al.* (DUNE Collaboration), arXiv:1512.06148.
[26] F. An *et al.* (JUNO Collaboration), J. Phys. G **43**, 030401 (2016).
[27] Y. Suzuki, arXiv:hep-ex/0110005.
[28] M. D. Kistler, H. Yuksel, S. Ando, J. F. Beacom, and Y. Suzuki, Phys. Rev. D **83**, 123008 (2011).
[29] T. Liu, B. Zhang, Y. Li, R. Y. Ma, and L. Xue, Phys. Rev. D **93**, 123004 (2016).
[30] K. Nakazato, E. Mochida, Y. Niino, and H. Suzuki, Astrophys. J. **804**, 75 (2015).
[31] J. H. Davis and M. Fairbairn, J. Cosmol. Astropart. Phys. 07 (2017) 052.
[32] C. Lunardini, Astropart. Phys. **79**, 49 (2016).
[33] S. Ando, K. Sato, and T. Totani, Astropart. Phys. **18**, 307 (2003).
[34] S. Ando and K. Sato, New J. Phys. **6**, 170 (2004).
[35] C. Lunardini, Phys. Rev. D **73**, 083009 (2006).
[36] L. E. Strigari, M. Kaplinghat, G. Steigman, and T. P. Walker, J. Cosmol. Astropart. Phys. 03 (2004) 007.
[37] M. Kaplinghat, G. Steigman, and T. P. Walker, Phys. Rev. D **62**, 043001 (2000).
[38] J. F. Beacom and M. R. Vagins, Phys. Rev. Lett. **93**, 171101 (2004).
[39] J. F. Beacom, Annu. Rev. Nucl. Part. Sci. **60**, 439 (2010).
[40] M. Malek *et al.* (Super-Kamiokande Collaboration), Phys. Rev. Lett. **90**, 061101 (2003).
[41] K. Bays *et al.* (Super-Kamiokande Collaboration), Phys. Rev. D **85**, 052007 (2012).
[42] H. Zhang *et al.* (Super-Kamiokande Collaboration), Astropart. Phys. **60**, 41 (2015).
[43] A. Priya and C. Lunardini, J. Cosmol. Astropart. Phys. 11 (2017) 031.
[44] L. Yang and C. Lunardini, Phys. Rev. D **84**, 063002 (2011).
[45] J. G. Keehn and C. Lunardini, Phys. Rev. D **85**, 043011 (2012).
[46] C. Lunardini, Phys. Rev. Lett. **102**, 231101 (2009).
[47] K. Nakazato, K. Sumiyoshi, H. Suzuki, and S. Yamada, Phys. Rev. D **78**, 083014 (2008); **79**, 069901(E) (2009).
[48] S. Nagataki, K. Kohri, S. Ando, and K. Sato, Astropart. Phys. **18**, 551 (2003).
[49] S. Nagataki and K. Kohri, Prog. Theor. Phys. **108**, 789 (2002).
[50] T. Fischer, S. C. Whitehouse, A. Mezzacappa, F.-K. Thielemann, and M. Liebendorfer, Astron. Astrophys. **499**, 1 (2009).
[51] K. Sumiyoshi, S. Yamada, and H. Suzuki, Astrophys. J. **688**, 1176 (2008).
[52] O. L. Caballero, G. C. McLaughlin, R. Surman, and R. Surman, Phys. Rev. D **80**, 123004 (2009).
[53] R. W. O'Shaughnessy, R. K. Kopparapu, and K. Belczynski, Classical Quantum Gravity **29**, 145011 (2012).
[54] M. Dominik, K. Belczynski, C. Fryer, D. E. Holz, E. Berti, T. Bulik, I. Mandel, and R. O'Shaughnessy, Astrophys. J. **779**, 72 (2013).
[55] J. Abadie *et al.* (LIGO Scientific and Virgo Collaborations), Classical Quantum Gravity **27**, 173001 (2010).
[56] B. P. Abbott *et al.* (LIGO Scientific and Virgo Collaborations), Phys. Rev. Lett. **119**, 161101 (2017).
[57] N. Gehrels *et al.* (Swift Science Collaboration), Astrophys. J. **611**, 1005 (2004); **621**, 558(E) (2005).
[58] N. R. Butler, D. Kocevski, J. S. Bloom, and J. L. Curtis, Astrophys. J. **671**, 656 (2007).
[59] H. Yüksel, M. D. Kistler, J. F. Beacom, and A. M. Hopkins, Astrophys. J. **683**, L5 (2008).
[60] H. Yüksel and M. D. Kistler, Phys. Lett. B **751**, 413 (2015).
[61] C. Lunardini and I. Tamborra, J. Cosmol. Astropart. Phys. 07 (2012) 012.
[62] Y. L. Zhu, A. Perego, and G. C. McLaughlin, Phys. Rev. D **94**, 105006 (2016).
[63] A. Malkus, A. Friedland, and G. C. McLaughlin, arXiv: 1403.5797.
[64] A. Malkus, J. P. Kneller, G. C. McLaughlin, and R. Surman, Phys. Rev. D **86**, 085015 (2012).
[65] S. Setiawan, M. Ruffert, and H.-Th. Janka, Mon. Not. R. Astron. Soc. **352**, 753 (2004).
[66] A. Perego, S. Rosswog, R. M. Cabezn, O. Korobkin, R. Kppeli, A. Arcones, and M. Liebendrfer, Mon. Not. R. Astron. Soc. **443**, 3134 (2014).
[67] W.-X. Chen and A. M. Beloborodov, Astrophys. J. **657**, 383 (2007).
[68] N. I. Shakura and R. A. Sunyaev, Astron. Astrophys. **24**, 337 (1973).
[69] S. L. Shapiro, Phys. Rev. D **95**, 101303 (2017).
[70] M. Shibata and K. Taniguchi, Phys. Rev. D **73**, 064027 (2006).
[71] M. Shibata, M. D. Duez, Y. T. Liu, S. L. Shapiro, and B. C. Stephens, Phys. Rev. Lett. **96**, 031102 (2006).
[72] F. H. Nouri *et al.*, Phys. Rev. D **97**, 083014 (2018)..
[73] R. Fernandez and B. D. Metzger, Mon. Not. R. Astron. Soc. **435**, 502 (2013).
[74] M. B. Deaton, M. D. Duez, F. Foucart, E. O'Connor, C. D. Ott, L. E. Kidder, C. D. Muhlberger, M. A. Scheel, and B. Szilagyi, Astrophys. J. **776**, 47 (2013).
[75] I. V. Artemova, G. Bjoernsson, and I. D. Novikov, Astrophys. J. **461**, 565 (1996).

[76] O. L. Caballero, T. Zielinski, G. C. McLaughlin, and R. Surman, Phys. Rev. D **93**, 123015 (2016).
[77] K. Hotokezaka, K. Kiuchi, K. Kyutoku, T. Muranushi, Y. i. Sekiguchi, M. Shibata, and K. Taniguchi, Phys. Rev. D **88**, 044026 (2013).
[78] Y. Sekiguchi, K. Kiuchi, K. Kyutoku, and M. Shibata, Phys. Rev. Lett. **107**, 051102 (2011).
[79] J. Lippuner, R. Fernndez, L. F. Roberts, F. Foucart, D. Kasen, B. D. Metzger, and C. D. Ott, Mon. Not. R. Astron. Soc. **472**, 904 (2017).
[80] S. L. Shapiro and S. A Teukolsky, *Black Holes, White Dwarfs and Neutron Stars* (Wiley, New York, 1983).
[81] F. Foucart, E. O'Connor, L. Roberts, M. D. Duez, R. Haas, L. E. Kidder, C. D. Ott, H. P. Pfeiffer, M. A. Scheel, and B. Szilagyi, Phys. Rev. D **91**, 124021 (2015).
[82] T. Totani, K. Sato, H. E. Dalhed, and J. R. Wilson, Astrophys. J. **496**, 216 (1998).
[83] K. Nakazato, K. Sumiyoshi, H. Suzuki, T. Totani, H. Umeda, and S. Yamada, Astrophys. J. Suppl. Ser. **205**, 2 (2013).
[84] K. Nakazato, Phys. Rev. D **88**, 083012 (2013).
[85] D. W. Hogg, arXiv:astro-ph/9905116.
[86] http://syntheticuniverse.org.
[87] M. D. Kistler, K. Z. Stanek, C. S. Kochanek, J. L. Prieto, and T. A. Thompson, Astrophys. J. **770**, 88 (2013).
[88] M. D. Kistler, H. Yüksel, and A. M. Hopkins, arXiv: 1305.1630.
[89] S. E. Woosley and A. heger, Astrophys. J. **752**, 32 (2012).
[90] B. D. Metzger, A. L. Piro, and E. Quataert, Mon. Not. R. Astron. Soc. **396**, 1659 (2009).
[91] S. E. de Mink and K. Belczynski, Astrophys. J. **814**, 58 (2015).
[92] B. P. Abbott *et al.* (LIGO Scientific and Virgo Collaborations), Astrophys. J. **832**, L21 (2016).